Results in Engineering 24 (2024) 102921

Contents lists available at ScienceDirect

Results in Engineering

journal homepage: www.sciencedirect.com/journal/results-in-engineering

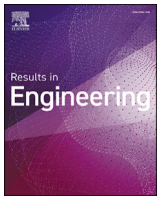

Research paper

Life extension of wind turbine drivetrains by means of SCADA data: Case study of generator bearings in an onshore wind farm

Kelly Tartt [a,b,*], Abbas Mehrad Kazemi-Amiri [a], Amir R. Nejad [b], James Carroll [a], Alasdair McDonald [c]

[a] Department of Electronic and Electrical Engineering, University of Strathclyde, Glasgow, G1 1XQ, UK
[b] Department of Marine Technology, Norwegian University of Science and Technology, Trondheim, NO-7491, Norway
[c] School of Engineering, University of Edinburgh, Edinburgh, EH9 3FB, UK

ARTICLE INFO

Keywords:
Wind energy
SCADA
Remaining useful life (RUL)

ABSTRACT

Accurate predictions for remaining useful life (RUL) of wind turbine drivetrains are crucial in reducing downtime, optimising maintenance strategies, extending operational life and improving costs. The purpose of this study is to present a method which utilises SCADA data for RUL estimation. It aims to answer whether, by only having the basic SCADA data, normally collected from all wind turbines, valuable RUL prediction results can be obtained. The work intends to develop a reliable, accurate, user-friendly and informative tool to enable observation of any growing trends in the proposed metrics, such as temperature difference, cumulative sum of temperature difference and the moving average of the cumulative sum. These metrics are defined based on the differences between the actual temperatures of the components, that might have undergone some damage and the model predicted temperatures of those components if they would have remained healthy, throughout years of operation. A machine learning model is used, along with selected SCADA input parameters, to predict the healthy state temperature of components. The proposed method is implemented on SCADA data collected from an actual wind farm over seven years. The results of this study show that while the SCADA data analysis can contribute to fault detection, the estimation of RUL purely based on SCADA appears to be uncertain. Such tools however, can be used as a monitoring method, during operation, to record abnormality trend of the components over the years and can be used as important inputs for the life extension evaluation of wind turbine drivetrains.

1. Introduction

The importance of investing in renewable energy such as solar, wind and hydro to name a few, has again been highlighted over the last few years due to a variety of reasons and continues to be a hot topic. One reason is the energy crisis [1], another is to ensure energy security and a third is that in order to achieve the various agreements, targets and policies set worldwide, such as the Paris Agreement [2], Net Zero [3] and REPowerEU plan [4], there needs to be a large and rapid increase in the renewable energy capacity. The International Energy Agency (IEA) states that within the next 5 years, 2400 GW of renewable energy needs to be installed, which is the same amount of capacity that has been installed over the last 20 years, in order to meet the set targets [5].

Wind and solar are leading the growth and it is predicted that by 2027, both wind and solar will provide almost 20% of power generation worldwide [5]. Looking specifically at wind energy, a report issued by Drax Electric Insights states that in the first quarter of 2023, electricity generated from wind power surpassed electricity generated from gas-fired power plants, for the first time ever in the UK [6]. The importance of both solar and wind energy, along with their potential growth is further highlighted by a number of feasibility studies, [7], [8] and economic analyses, [9], [10], that have been conducted. Proton exchange membrane (PEM) fuel cells is another area which has also been investigated, [11] and [12], along with turbine power plants [13].

According to the Global Wind Energy Council's (GWEC) Global Wind Report 2023, the total wind energy capacity currently stands at 906 GW, with 680 GW expected to be installed by 2027 [14]. 906 GW equates to over 300,000 wind turbines, both onshore and offshore, located worldwide.

A wind turbine's drivetrain, which is housed within the nacelle, is known as the "heart" of the turbine and is extremely important for the

* Corresponding author at: Department of Electronic and Electrical Engineering, University of Strathclyde, Glasgow, G1 1XQ, UK.
E-mail addresses: kelly.tartt@strath.ac.uk, kelly.tartt@ntnu.no (K. Tartt).

https://doi.org/10.1016/j.rineng.2024.102921
Received 1 April 2024; Received in revised form 8 September 2024; Accepted 16 September 2024
Available online 23 September 2024

wind turbine's operation. This is because the drivetrain contains all the equipment, which is responsible for converting kinetic energy from the wind turning the rotor blades, to electrical energy supplying the electrical grid. Therefore, any failures within the drivetrain can have severe consequences, so the reliability and smooth continuous operation of these turbines are important. In order to ensure the smooth production of power with minimum downtime, the operations and maintenance of the turbines are all important aspects to continuously monitor, review and modify.

One method used to monitor the turbines is via supervisory control and data acquisition (SCADA), [15]. All wind turbines are fitted with a number of sensors, in a variety of locations throughout the turbine and the average value over, typically each ten minute period and one second in some modern turbines, is recorded. SCADA data includes but is not limited to information such as wind speed, wind direction, power and temperature. Temperature measurements can include: ambient, nacelle, main bearing, gearbox, generator etc. Then based on the data recorded, owner/operators can make decisions with regards to the operations and maintenance, to ensure optimum power production and minimum downtime.

Due to the fact that SCADA data can be obtained from all turbines, methods of detecting failures and predicting a component's end of life using solely SCADA data, can be extremely beneficial, useful and cost effective, since they do not add any additional sensors.

As discussed in an earlier paper [16], the first stage of the proposed methodology to determine lifetime extension is data collection. It suggests that the amount of data collected affects the accuracy of the results and this paper aims to determine if by having the minimum amount of data available, useful results can still be obtained, regarding a component's end of life.

Accurately predicting a component's end of life can provide a number of advantages, such as enabling maintenance strategies to be optimised, reducing the amount of downtime the wind turbine can be subjected too and more cost-effective wind turbine operations.

Determining remaining useful life (RUL) and life extension evaluation are related but slightly different processes used in asset management, [17]. RUL can be defined as the estimated amount of time a component or system will continue to operate, until it fails. Whereas life extension evaluation investigates whether a component or system will continue to operate beyond it's specified life expectancy. Therefore, by finding the remaining useful life of a component or system, it can be determined whether this component or system will operate past it's specified lifetime.

The typical indicators of component failure, are an increase in temperature and vibration. Temperature measurements are readily available within the SCADA data, whereas vibration data is only typically part of condition monitoring. Therefore, temperature data will be used for this work.

A vast amount of research has already been carried out investigating the use of vibration data for failure detection but in addition to this, research into numerous models which can use SCADA data has also been carried out, specifically temperature data, as the input to predict failures and this is shown in Section 2. Therefore, the objective of this paper is not to 'reinvent the wheel' and develop another model but to develop a method for an informative tool, which uses SCADA data along with an existing, straightforward model, to detect any temperature changes or trends within certain drivetrain components, which can be used for life extension evaluation. The method will suggest which SCADA input parameters and model provide the most accurate predictions and how to display the results. The method aims to be comprehensive, informative and easy to implement. Real life data collected from a wind farm will be used to test the method. Moreover, the contribution/novelty of this work is to provide detailed documentation of the process, to support the evaluation of life extension.

The rest of this paper is structured as follows: Section 2 details existing research, Section 3 firstly describes identifying which model is a good predictor and then describes how to identify any trends in a component, which indicate that it is reaching it's end of life. Section 4 documents the results, along with a discussion, Section 5 contains the conclusions and Section 6 explains the future work.

2. Background and literature

A large amount of research has already been carried out using vibration data for failure prediction of wind turbine drivetrains, Turnbull et al. [18,19], Gómez et al. [20], Joshuva and Sugumaran [21], Igba et al. [22], Hussain and Gabbar [23], Teng et al. [24], Zhang et al. [25], to name a few because it has been proven to be more efficient/reliable. It was also mentioned earlier, that by using temperature data to determine the remaining useful life or fault detection of either a component within the drivetrain or the complete system, would be extremely beneficial because temperature data is typically readily available as part of the SCADA data. With this in mind, extensive research has previously been carried out investigating a variety of methods, although Carroll et al. [26] found that simple trending using temperature rarely highlighted potential failures. Yang et al. [27] also mentions that because SCADA data varies "over wide ranges under varying operational conditions", then without "an appropriate data analysis tool" it is difficult to detect faults from raw SCADA data. A Condition Monitoring technique based upon certain SCADA data correlations was proposed, in which it was concluded by Yang et al. [27] worked well in detecting faults within the drivetrain.

Murgia et al. [28] investigated the suitability of using SCADA-based condition monitoring, in order to diagnose faults within a wind turbine, by analysing temperature data. They used normal-behaviour modelling and identification of a threshold value and concluded that it is "suitable for individuating occurring drivetrain faults with at least months of advance, provided that qualifying points are addressed".

In another example, a normal behaviour model based upon an artificial neural network (ANN), using SCADA data has been proposed and tested on twelve wind turbines by Encalada-Dávila et al. [29] and it showed that main bearing faults could be detected several months in advance. A "state prediction approach" was used by Herp et al. [30], which was based on "bearing temperature residuals" along with Gaussian processes. This method was able to predict a failure approximately one month before failure. In addition, Dai et al. [31] looked at four different assessment criteria for assessing the performance of an ageing asset. One of the assessment criteria used the main bearing temperature data, it looked for changes and processed this data using Kernel Density Estimation.

The most commonly used data-driven models include support vector machines, neural networks, probabilistic models and decision trees according to Pandit et al. [32]. They explain that condition monitoring based on SCADA data "targets secondary effects of the fault". They discuss that the model's accuracy can be increased with feature selection and extraction but that it is a fine line to avoid over-fitting.

With regards to gearbox failures, a gearbox planetary stage failure was detected by monitoring gearbox oil temperature, power output and rotational speed in Feng et al. [33]. Whereas based on the first law of thermodynamics a relationship between temperature, efficiency, and either the power output or rotational speed was established by Feng et al. [34]. A new algorithm was then developed to detect gearbox failures based on both oil and bearing temperature measurements. It was concluded that the simple algorithms worked well in providing early warnings of gearbox failures. A Multivariate State Estimation Technique (MSET) was used by Yongjie et al. [35], along with the Moving Window Calculation (MWC). Where the MSET was used to estimate the gearbox temperature and the MWC used to get the dynamic trend of the average value of the differences between the estimated and real values. This paper concluded that the method was effective in detecting any anomalies. Moreover, thermal modelling, as well as thermal modelling combined with machine learning was investigated by Corley et al. [36]

and Corley et al. [37] respectively, where it was found that thermal modelling of the gearbox detected a fault, whereas nothing was obvious with just the temperature differences. Zhao and Zhang [38] used a prediction method, using temperature to detect faults by comparing the actual running condition of the gearbox, with the predicted condition and flagging any deviation. Gearbox oil temperature was used by Zeng et al. [39] in an anomaly detection method, based on the Sparse Bayesian Learning and hypothesis testing. A Support Vector Machine (SVM) regression model along with SCADA parameters was used to model the gearbox oil temperature by Zhang and Qian [40] and it was concluded that a warning approximately ten days before the fault was achieved. A deep neural network algorithm was "applied to model the lubricant pressure" by Wang et al. [41] and it was found that gearbox failures could be predicted approximately two to three days in advance. They also concluded that monitoring lubricant pressure provided more accurate results than monitoring gearbox oil temperature.

Specifically tested on a generator rear bearing, Hu et al. [42] established a performance degradation model using the Wiener process, with the maximum likelihood estimation method used for the model parameters. The "temperature trend data" was determined from the "relative temperature data" using the moving average method. It also established a remaining useful life (RUL) prediction model, based on the inverse Gaussian distribution. It was concluded that both the degradation model and prediction method were very effective with calculating remaining useful life.

Sudden fault detection of generator bearings was investigated by Velásquez [43]. They firstly used a multi-stage approach consisting of multiple regression models, then probability scores, a search grid validation and then the validated results were ran through "finite element modeling, boroscopy, and vibration analysis". They concluded that failures could be detected five days prior to vibration analysis, with a high accuracy.

Although not related to wind turbines, Apribowo et al. [44] used machine learning models such as an extreme gradient boosting algorithm, along with a temperature variable to predict the RUL of battery energy storage systems. It was concluded that this method provided accurate results.

Based on the existing literature, the main advantages of using SCADA data to estimate RUL are: that SCADA data is available from all wind turbines and there is typically a continuous flow of data. Whereas the main disadvantages are: the frequency resolution is lower when compared to condition monitoring and the type of data recorded may vary across turbines. Additional issues can also include: noise which may affect the SCADA data values, sensor failures or malfunctions which may cause gaps in the data due to turbine or equipment downtime, ensuring that the most relevant features or values are selected so that an accurate/reliable prognosis can be obtained, negotiating large volumes of data. As mentioned earlier, early fault detection is important, whereas using SCADA-based wind turbine condition monitoring to detect faults early can be challenging, due to subtle changes in the data.

The majority of the existing research summarised above looked at methods using quite complicated data-driven techniques, which has the advantage of providing more effective RUL predictions. Although, it was determined that the failures could only really be predicted a few months in advance, as a best case scenario, due to relying solely on temperature data, whereas using vibration data or a combination of both could predict failure much earlier.

The main aim of this work is to develop a method or process, in which a readily available machine learning model is proposed and utilised along with specific SCADA data input parameters, in order to obtain insight into a component's condition. This method or process will try and establish some indicators to help track the condition of components and flag up a warning when a component is coming to the end of it's life, then ideally these indicators could be used to compare components across multiple turbines. Therefore, the advantage of this work is that it provides a comprehensive but straight-forward method/process for determining a component's end of life based on SCADA temperature data.

3. Methodology

3.1. Selecting a suitable model predictor

The first stage is to determine which model is a reliable and easy to use predictor. A flowchart detailing the method of determining a suitable model predictor is shown in Fig. 1.

To start this process, labeled data is needed, meaning that "healthly" data is required first to build a model.

Prior to passing any data into the model, the first step is to filter the data, as shown in Step 1 in Fig. 1. This includes removing any missing values and replacing any negative power values with the previous or nearest positive value.

Following this step, the nacelle ambient temperature, T_{na}, is then deducted from the chosen component temperature, T_c, (Step 2), in order to normalise all the component's temperature values, T_{norm}.

$$T_{norm} = T_c - T_{na} \tag{1}$$

The next step (Step 3) begins with selecting the input parameters based upon the chosen model, for example, linear regression and polynomial regression models typically only accept one input parameter, along with the component temperature values, whereas the support vector machine model and regression tree ensemble model can accept multiple input parameters. Once the parameters have been selected, any data points that are found to be more than three (3) standard deviations from the mean are removed, as the final filtering process. The "healthy" data is then randomly split into 70% training data and 30% test data.

The data is then passed through the model, in order for the model to determine the predicted component temperatures, as the output.

The simplest regression model, which is the linear regression model, was deemed not to be suitable due to the fact that the correlation between power and temperature is not linear, so instead the following models are selected:

1. Polynomial Regression Model.
2. Support Vector Machine (SVM) Model.
3. Regression Tree Ensemble Model.

From the results/model output, the correlation coefficient between the actual and predicted temperature values are calculated. If the correlation coefficient is low, the process is repeated using different input parameters and/or models, until a respectable correlation coefficient is achieved. A correlation coefficient of 0.8 is shown in Step 3 in Fig. 1 and this has been chosen because any value equal to or above 0.8, is assumed to be highly correlated, [45].

Graphs are also plotted to visualise the correlation, they include: temperature vs. power, actual vs. predicted temperature and temperature vs. time.

This process is then repeated using the whole "healthy" data set to both train and test the model. The results from this process are also plotted to see the model sensitivity.

Due to the sheer amount of data, the daily mean values are calculated for each parameter, i.e. the power, actual component temperature and predicted component temperature. This data is then used to produce more graphs to analyse the correlation, to determine if this is a suitable model.

As mentioned above, the first model selected is the polynomial regression model to the eighth order. Power and then torque, along with the component temperature values in the training data set are used as the input parameters to train the model, before the power or torque values in the test data set are used to predict the component temperature values.

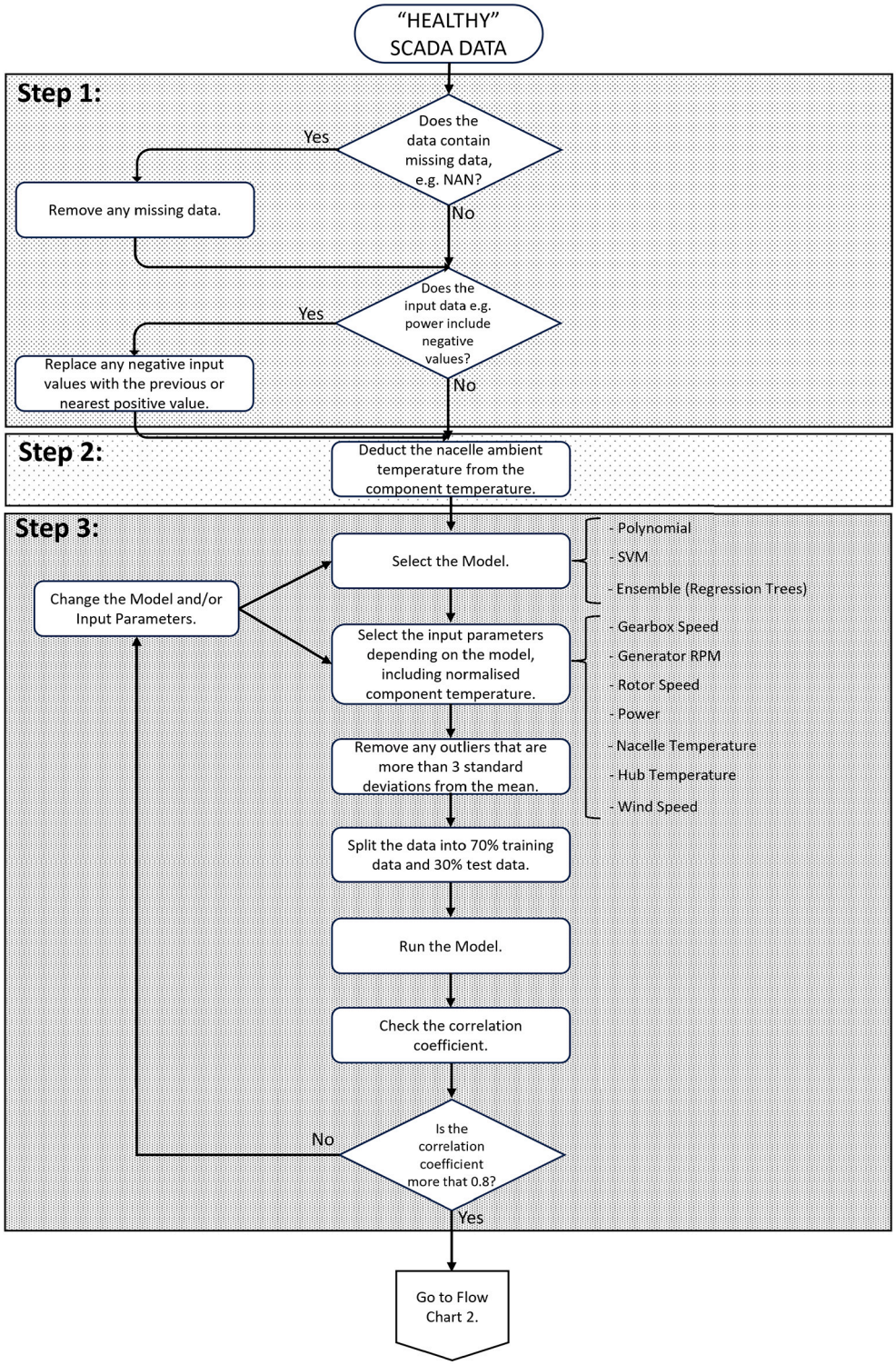

Fig. 1. Flow chart showing how to select a suitable model predictor.

The next model investigated is the support vector machine model, mainly because this model can accept multiple inputs. Therefore, the same process is followed as described above, using firstly power as the only input parameter and then power along with rotor speed as the input parameters.

Next the regression tree ensemble model is used, again due to the fact that multiple input parameters can be used. Initially, seven different parameters are selected along with the component temperature, these include: power, rotor speed, generator RPM, gearbox speed, nacelle temperature, hub temperature and wind speed. Various combinations are used along with the model to determine which parameters give the best fit.

Upon completion of this process, the next step is to implement the model to assist with identifying components reaching their end of life, which is described in Section 3.2.

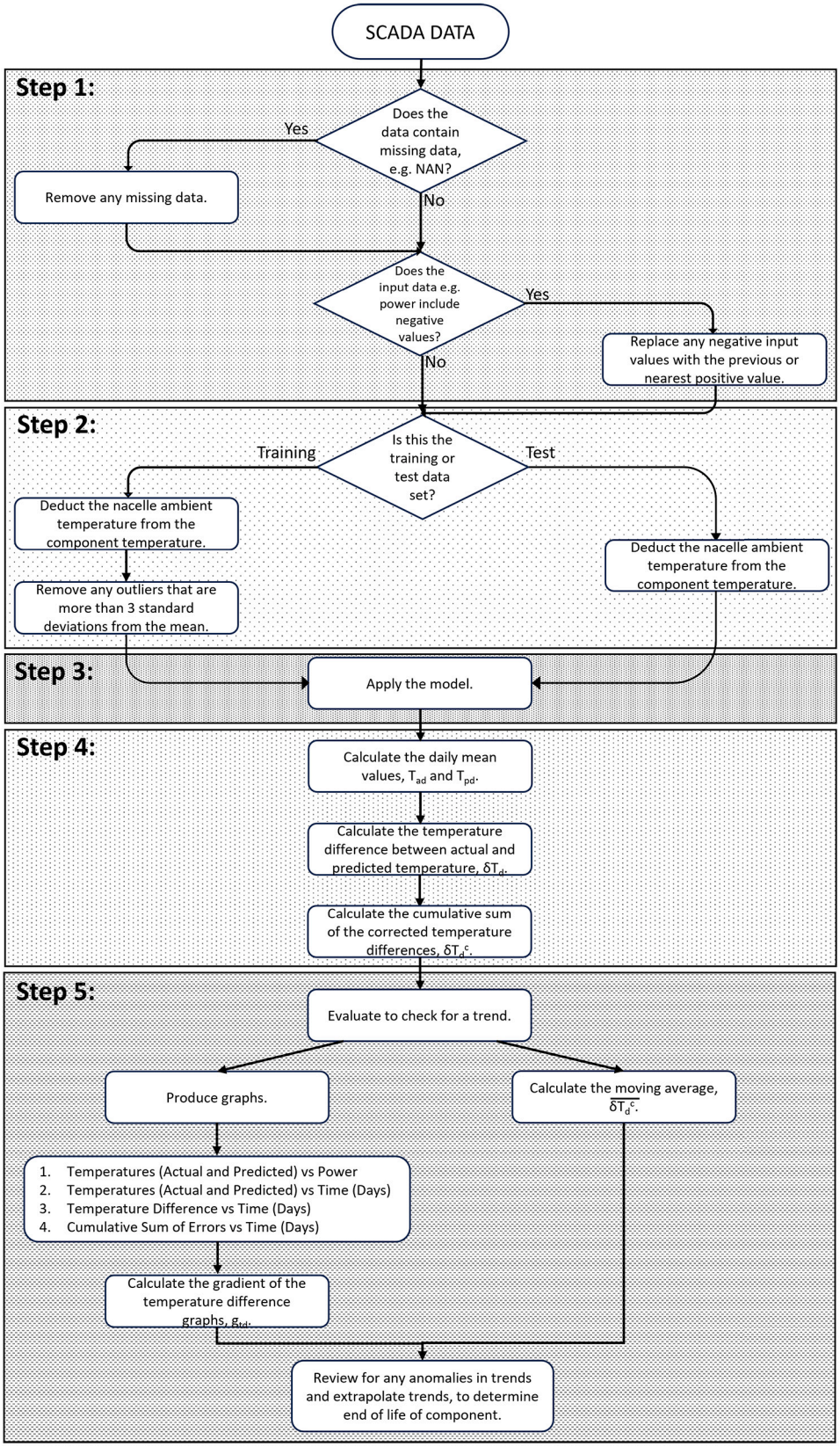

Fig. 2. Flow chart showing method used for identifying critical components in the drivetrain.

3.2. Identifying critical components in the drivetrain

The critical components, those which may fail earlier, need to be identified. One way to do this is to review the failure data but if this is not available, then vulnerability maps may be used, such as the ones produced by Nejad et al. [46], Nejad et al. [47] and Tartt et al. [48].

The proposed method to try and identify components reaching their end of life, is summarised in a flowchart shown in Fig. 2.

The first step is to collect all the SCADA data from the first turbine. The pre-processing discussed in Section 3.1 and as shown in Steps 1 and 2 in the flow chart (Fig. 2), is carried out on both the training and test data. In this method, the training data used for the model is all of the "healthy" data, which is typically the turbine's first year of operation and the test data is all the data collected in a subsequent year. The pre-processing of both the training and test data includes: removing any missing data, replacing any negative power values with either the previous or nearest positive value, as well as deducting the nacelle ambient temperature from the component temperature. As mentioned in Section 3.1, the nacelle ambient temperature is deducted from the component temperature, in order to normalise the temperature values. An additional pre-processing step for the training data, is to remove any outliers that are more than three (3) standard deviations from the mean.

Once the SCADA data has been pre-processed, the selected input parameters are then passed into the model (Step 3). From Section 3.1, the regression tree ensemble model, using three input parameters from the SCADA data: power, rotor speed and nacelle temperature, along with the component temperature, are the model and input parameters that are shown to be the best predictor.

From the results obtained, the daily mean values of power, actual component temperature, T_{ad_j} and predicted component temperature, T_{pd_j}, for each day, j, are calculated from the instantaneous values of actual and predicted temperature, T_{a_i} and T_{p_i}, respectively, as shown in Equations (2) and (3) (Step 4), where n refers to the number of ten minute blocks per day (i.e. 6 blocks in one hour, 24 hours a day, therefore n = 6x24 = 144).

$$T_{ad_j} = \frac{\sum_{i=x}^{x+(n-1)} T_{a_i}}{n} \tag{2}$$

$$T_{pd_j} = \frac{\sum_{i=x}^{x+(n-1)} T_{p_i}}{n} \tag{3}$$

The daily temperature difference, δT_{d_j}, is then calculated as shown in Equation (4).

$$\delta T_{d_j} = T_{ad_j} - T_{pd_j} \tag{4}$$

Once the temperature difference is determined, the cumulative sum of the temperature differences, $\delta T^c_{d_M}$, can then be calculated as per Equation (5), where M equals the corresponding time, in this case the day. Calculating the cumulative sum of the temperature differences between the actual and predicted temperatures, is a straightforward way to highlight anomalies or change in trends, which then forces further investigation.

$$\delta T^c_{d_M} = \sum_{j=1}^{M} \delta T_{d_j} \tag{5}$$

One evaluation method is to plot graphs, therefore, various graphs are then plotted using both the temperature difference and cumulative sum values against the time in days. These graphs are then reviewed for anomalies and to determine if any trends are present, which would assist in determining the end of life of the component (Step 5).

The next analysis carried out, is the calculation of the gradient of the temperature difference, g_{td}, graphs, for all the turbines, to see whether the closer you get to the failure, the gradient of the temperature difference increases.

$$g_{td} = \frac{(\delta T_{d_j+1} - \delta T_{d_j})}{(t_{j+1} - t_j)} \tag{6}$$

Initially the gradient over each day is determined, i.e. $t_{j+1} - t_j = 1$, as shown in Equation (6), then the average over five, ten and thirty days are calculated.

Another method used to help identify any trends, is the moving average method. Therefore, the final analysis to be carried out is a similar method to the one used to calculate the moving average, $\overline{\delta T^c_{d_M}}$, and that is to divide the cumulative sum on any day, $\delta T^c_{d_M}$, by the number of days until then, t_M, as shown in Equation (7).

$$\overline{\delta T^c_{d_M}} = \frac{\delta T^c_{d_M}}{t_M} \tag{7}$$

Following a repair, the cumulative sum is reset. This analysis is to try and see if a threshold value can be determined, in which if any turbine appears above this threshold, then a drivetrain component maybe coming to the end of it's life. It may be defined as an average accumulation of temperature difference.

This model/process is then repeated for all years, with the subsequent years as the test data, keeping data from the "healthy" year as the training data set, as well as on all the remaining turbines.

3.3. Case study

3.3.1. Data set

Data from the Kelmarsh Wind farm is used for the case study [49]. The Kelmarsh wind farm is located in Northamptonshire (see Fig. 3) and consists of six (6) onshore 2.05MW Senvion MM92 wind turbines [50]. The SCADA data has been collected over a seven (7) year period, from 2016 to the end of 2022. Status reports/data logs are also available. The data logs show two (2) faults occurred within the generators during 2022, one in Turbine 2 and one in Turbine 4. Knowing that a fault

Fig. 3. Location of Kelmarsh wind farm.

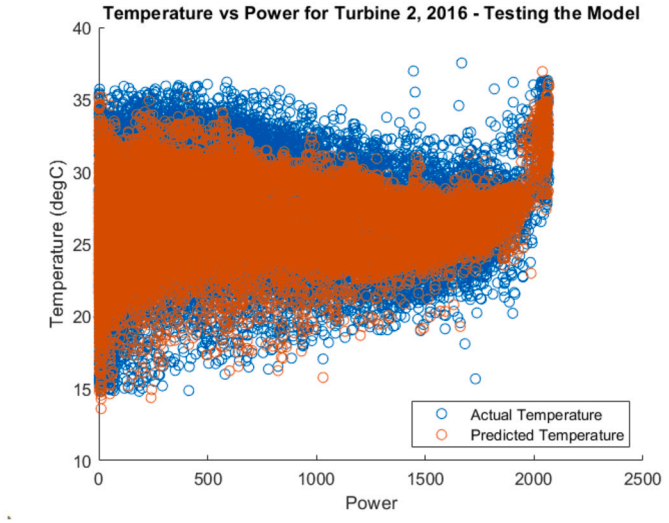

Fig. 4. Testing the model - temperature vs. power.

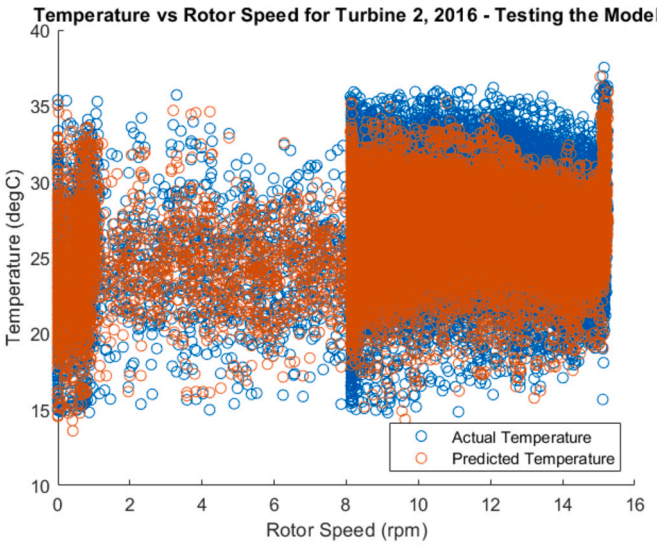

Fig. 5. Testing the model - temperature vs. rotor speed.

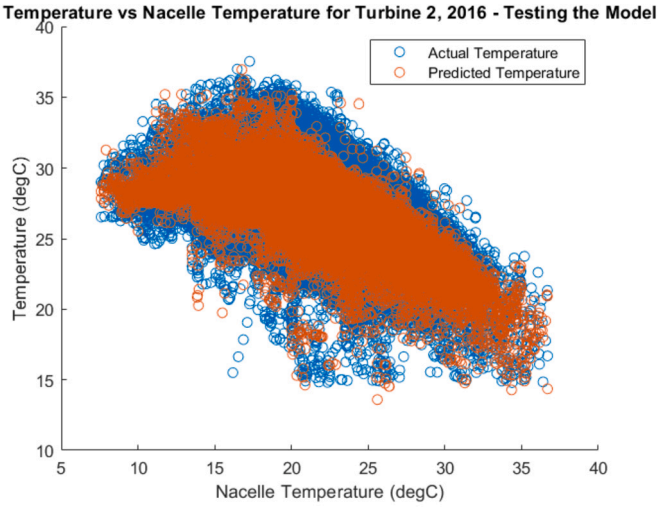

Fig. 6. Testing the model - temperature vs. nacelle temperature.

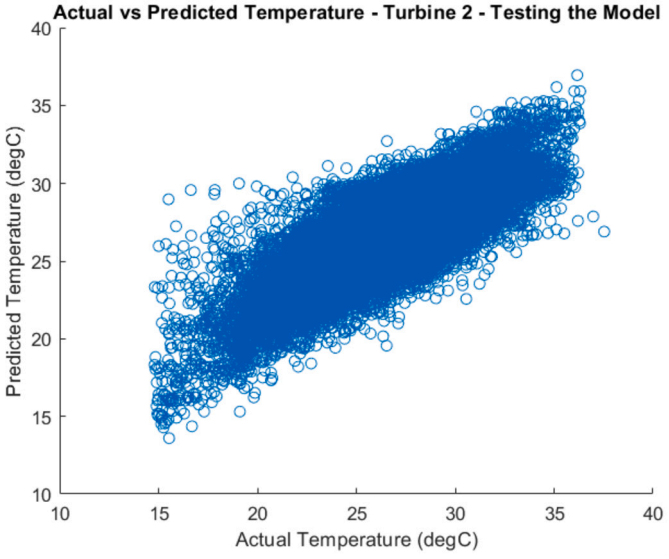

Fig. 7. Testing the model - actual vs predicted temperature.

occurred and in which component, is extremely useful for evaluation of the proposed approach of life extension described here.

3.3.2. Implementation

The methods described in Sections 3.1 and 3.2, are implemented using this data set. The SCADA data from the year 2016 is used as the training data set and the test data set are each of the subsequent years.

Initially, the method/model is run on each component, including the generator rear bearing, generator front bearing, front bearing, rear bearing and gear oil inlet, for each year and each turbine. This is to see if any one component is following a different trend, which may indicate that it may be approaching it's end of life.

Due to the fact that the data logs record failures in the generator non-drive end (NDE) bearing, we would expect the generator rear bearing to follow a different trend to the rest.

4. Results and discussion

This section displays the results produced when using the data set in Section 3.3.1 with the methods described in Sections 3.1 and 3.2.

4.1. Selecting a suitable model predictor

Figs. 4–8, show the fit or correlation of the regression tree ensemble model used. These are the results that are produced when all the data in the 2016 data set for one of the turbines, are used to both train and test the model. Fig. 4 shows both the actual and predicted temperatures against power, which is one of the input parameters used. Fig. 5 illustrates both the actual and predicted temperatures against rotor speed and Fig. 6 displays the temperatures against the nacelle temperature, which are the other two input parameters. Fig. 7 presents the actual temperature against the predicted temperature and Fig. 8 shows both the actual and predicted temperatures per day.

4.2. Identifying critical components in the drivetrain

As mentioned previously, the method described in Section 3.2 is implemented upon a data set consisting of six wind turbines, spanning seven years and the results are discussed below.

Section 3.3.2 discussed implementing the method on each component, including the rear generator bearing, front generator bearing, front bearing, rear bearing and gear oil inlet within each turbine and Figs. 9 and 10 show the results for Turbine 4. The results for the other five turbines can be found in Appendix B (see Figs. B.28–B.37).

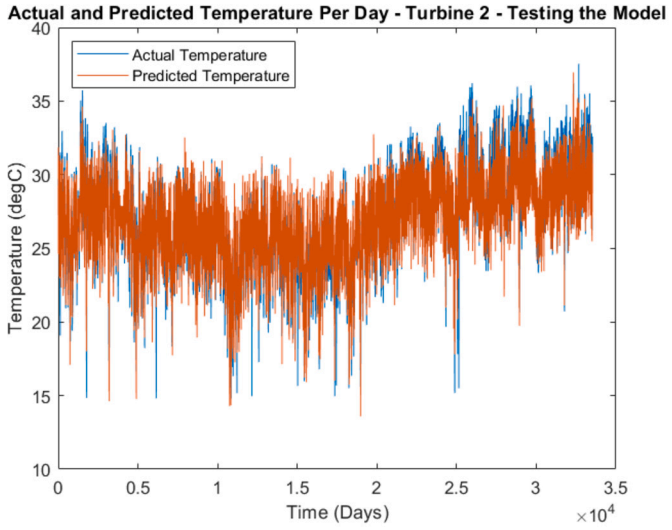

Fig. 8. Testing the model - comparing the actual vs predicted temperature.

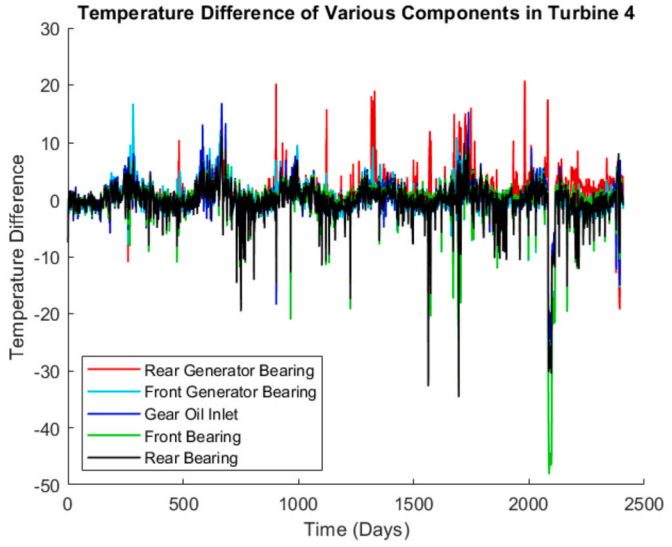

Fig. 9. Temperature differences for various components in Turbine 4.

Fig. 9 shows the temperature differences of the various components in Turbine 4 and Fig. 10 shows the cumulative sum of the temperature differences of the various components in the turbine.

The cumulative sum graph (Fig. 10) shows that the rear generator bearing appears to follow a different trend to the other components. This trend is the same across all turbines, which corresponds well with the status reports indicating failure of these components later on. Therefore, the rear generator bearing is chosen for further investigation in this paper.

All the results for the rear generator bearing will now be collected and compared. The graphs shown in Figs. 11 and 12, present both the temperature difference and cumulative sum of the temperature difference respectively, for all six turbines between the years 2016 and 2022.

Fig. 11 shows that the biggest differences in temperature occurred in Turbines 1 (red), 2 (cyan), 4 (green) and 6 (black). The status reports confirmed that in 2022, the generator NDE bearing failed in Turbines 2 and 4, so it is expected that the actual component temperature would be higher than the predicted temperature in these turbines. Fig. 12 shows that the six turbines appear to split into two groups, the first group consists of Turbines 1, 4 and 6 and the second group consists of Turbines 2, 3 and 5. The first group has a much higher cumulative sum than the second group and they appear to split into the separate groups around day

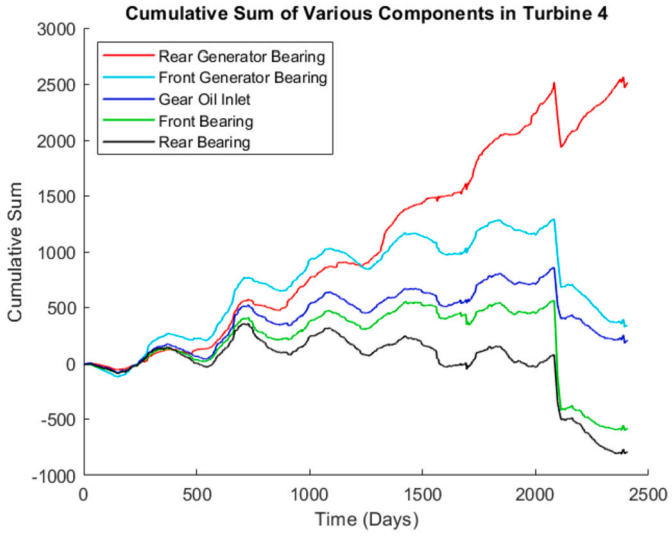

Fig. 10. Cumulative sum of the temperature differences for various components in Turbine 4.

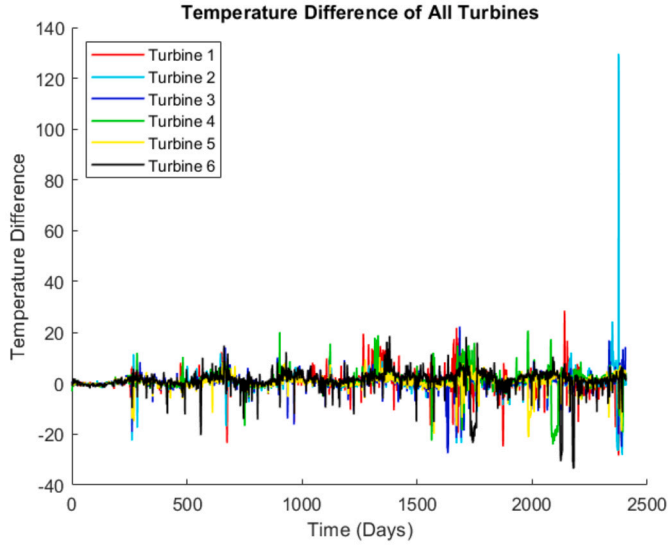

Fig. 11. Temperature differences for all turbines over all years.

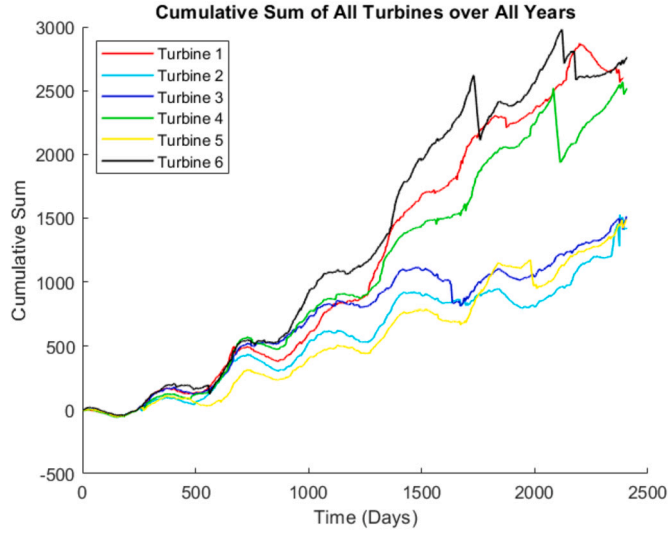

Fig. 12. Cumulative sum of the temperature differences for all turbines over all years.

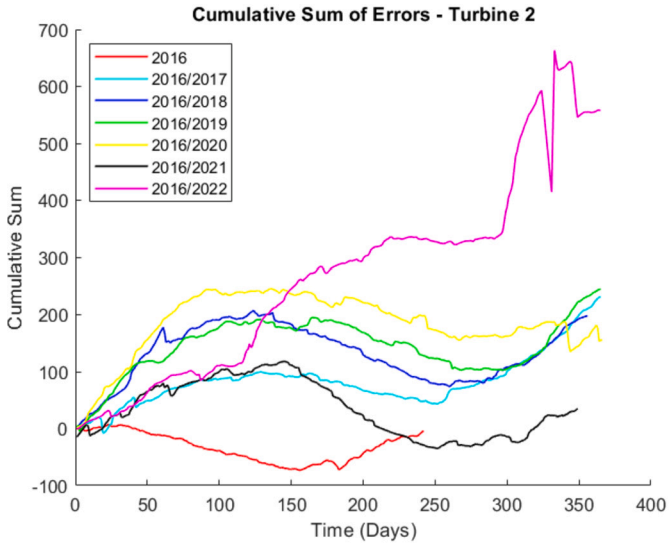

Fig. 13. Turbine 2 - Cumulative sum of the temperature differences.

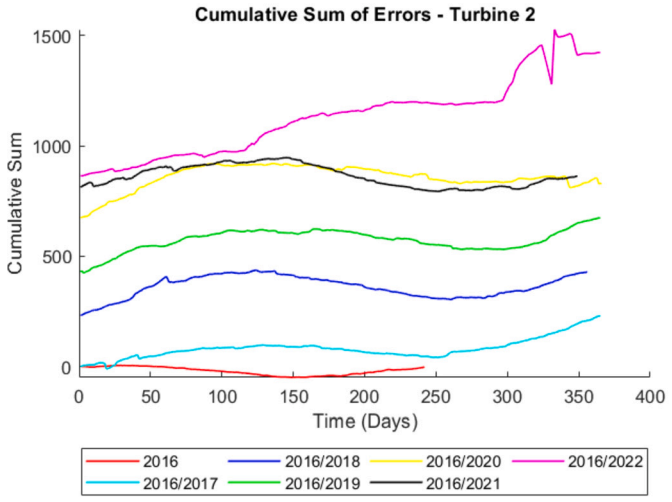

Fig. 14. Turbine 2 - Cumulative sum of the temperature differences continuing from previous year.

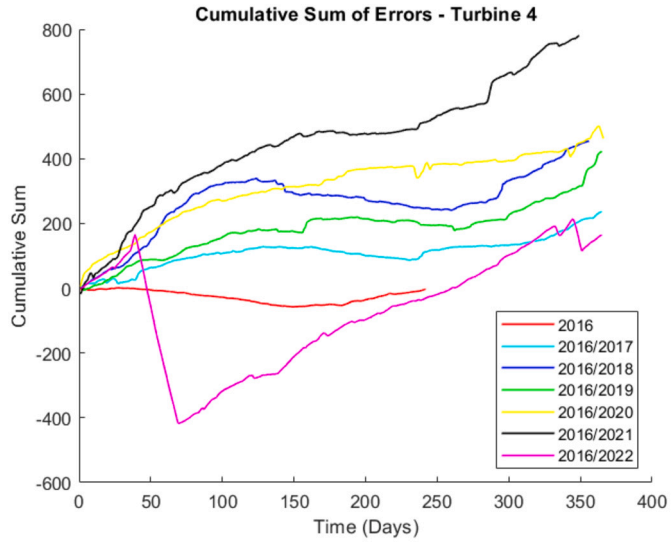

Fig. 15. Turbine 4 - Cumulative sum of the temperature differences.

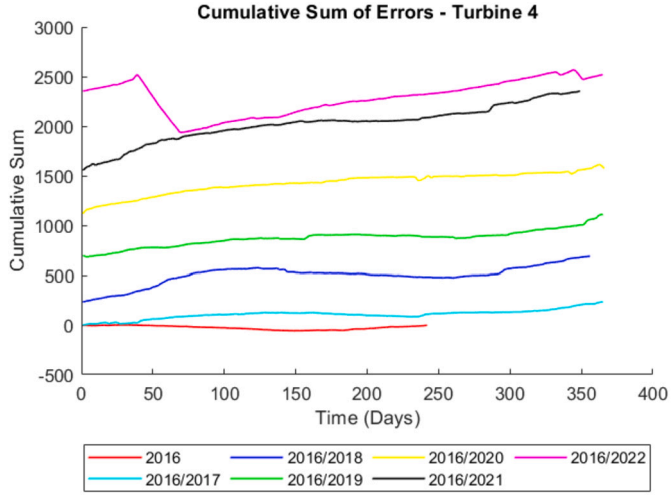

Fig. 16. Turbine 4 - Cumulative sum of the temperature differences continuing from previous year.

1000, which corresponds to the first quarter of 2019. Again, Turbines 1 and 6 follow the trend similar to Turbine 4, which had a generator NDE bearing failure, so it appears that these two turbines also had some issues, which will be discussed later.

The results from each turbine are now plotted individually to identify any further trends.

The graphs in Figs. 13, 15 and 17, show the cumulative sum of the temperature difference between the actual and predicted rear generator bearing temperature values for Turbines 2, 4 and 1, starting from zero at the start of every year, whereas Figs. 14, 16 and 18, show the cumulative sum of the difference in actual and predicted temperatures, that are a continuation from the previous year. Both styles of graphs have been shown, in order to show that no matter how much data is available, whether it is only a few years which would mean the graph starts from zero or many years meaning a continuation between the years can be plotted, any anomalies or trends can be seen. The graphs for the remaining three turbines can be found in Appendix C.

Starting with Turbine 2, in which it is known that a generator NDE bearing failure has occurred, it can be seen from both Figs. 13 and 14, that there is an obvious trend change in 2022. This wasn't seen as clearly in Fig. 12 but there was a large change in temperature observed in Fig. 11 towards the end of 2022. From Table A.1, the scheduled downtime occurred in the second half of November 2022, which matches the findings shown in the graphs. The trend appears to initially change around day 120 in the year 2022, which is approximately 200 days before the failure occurred. Then there is another change at around day 300.

With regards to Table A.1, which can be found in Appendix A along with Table A.2, this table shows a summary of the scheduled maintenance for each turbine over the last three years and Table A.2 shows a summary of the forced outage for each turbine over the last three years. This data has been taken from the status files, which were included with the turbine data files. The tables show the total number of downtime hours over the year per turbine, along with the maximum number of hours in any one occurrence, along with the month it occurred, when the total number of hours was above fifty.

The next turbine in which it is known that a generator NDE bearing failure has occurred is Turbine 4. There is an obvious rising trend for Turbine 4 in year 2021 (Fig. 15). The cumulative sum in this year is significantly different and higher than the other years, followed by the continuation of the increasing trend in early 2022 (Fig. 16) when the failure has occurred and been reported in the log documents/status reports. Table A.1 shows the downtime occurred in February 2022, with the replacement taking place in March 2022.

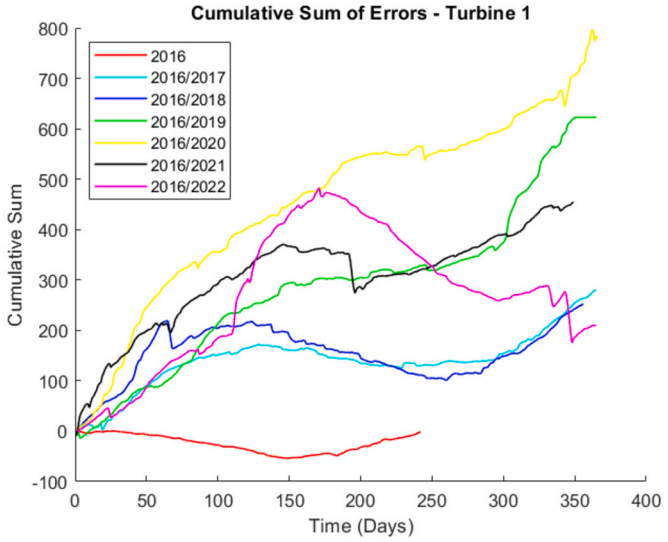

Fig. 17. Turbine 1 - Cumulative sum of the temperature differences.

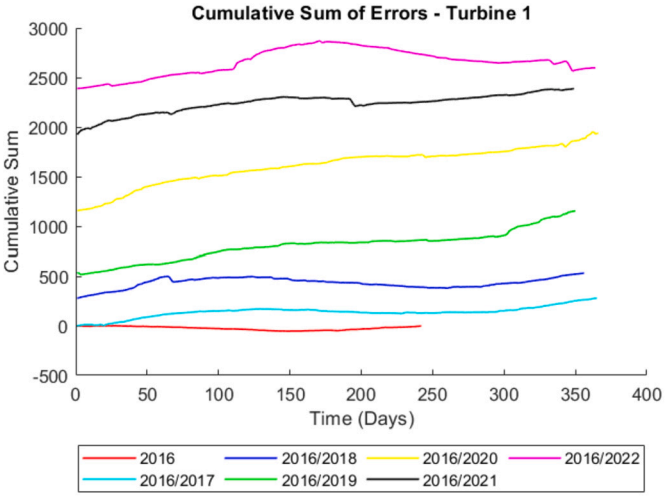

Fig. 18. Turbine 1 - Cumulative sum of the temperature differences continuing from previous year.

Figs. 17 and 18 show the results for Turbine 1. Turbine 1 is one of the turbines which shows a trend similar to Turbine 4 in Fig. 12, which is known to have had a bearing failure. The abnormal higher operating temperature of the rear generator bearing in this turbine starts to appear towards the end of 2019 (Fig. 17). This becomes more obvious in 2020 (Fig. 17), whose trend shows a surge in cumulative sum in Fig. 17. This rise in operating temperature continues in year 2021, which is more obvious in Fig. 18, as the continued cumulative sum is higher than the previous year. This is followed by a sharp rise in year 2022 (a sudden change in trend compared to the past years about day 120 onwards), leading to the scheduled downtime as reported in the log documents/status reports. The log documents/status reports show there was a scheduled downtime in June 2022, due to the proactive replacement of the NDE bearing. This is the same bearing that failed and had to be replaced in Turbines 2 and 4.

Figs. 19–24, show plots of the annual cumulative sum values (reset to zero and continued) in six separate figures, for years 2020, 2021 and 2022, respectively. Each figure corresponds to one year but includes all turbines. These compare the cumulative sum values and demonstrate those with higher temperature cumulative sum values, will be more susceptible to failure.

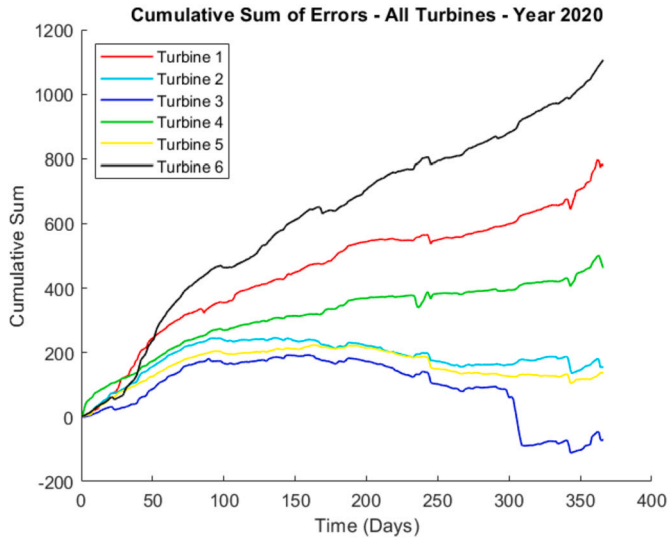

Fig. 19. All turbines - Cumulative sum of the temperature differences for year 2020.

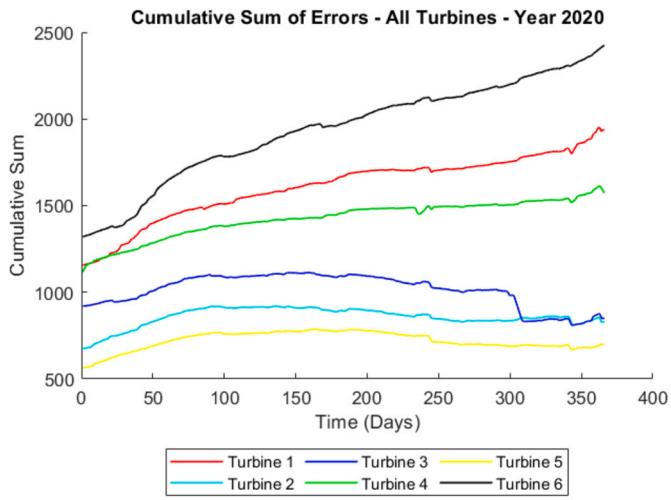

Fig. 20. All turbines - Cumulative sum of the temperature differences continuing from previous year for year 2020.

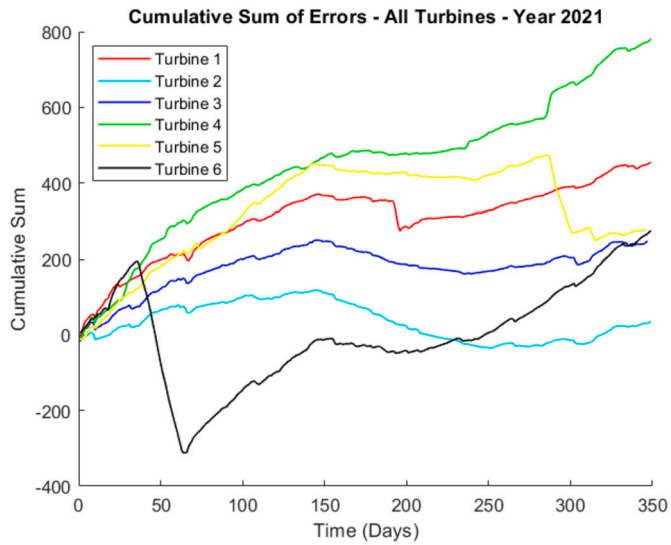

Fig. 21. All turbines - Cumulative sum of the temperature differences for year 2021.

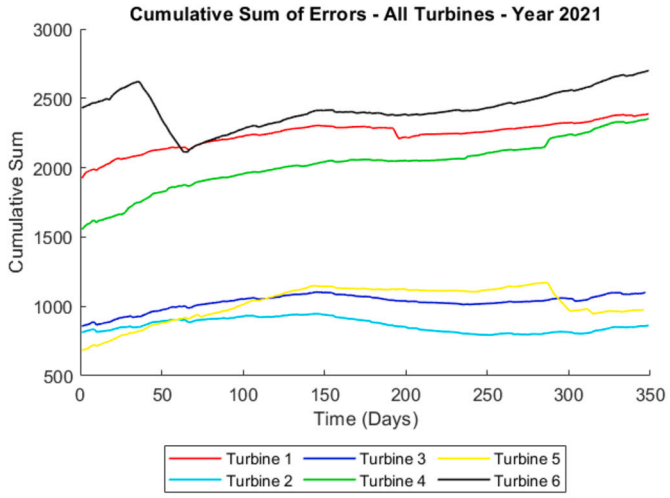

Fig. 22. All turbines - Cumulative sum of the temperature differences continuing from previous year for year 2021.

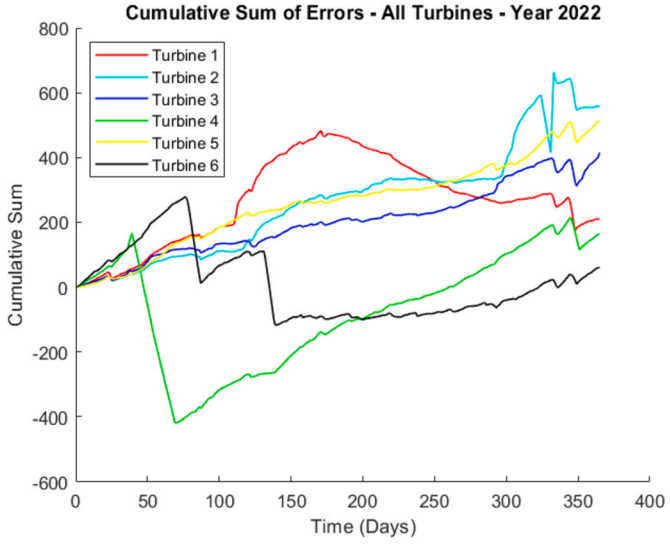

Fig. 23. All turbines - Cumulative sum of the temperature differences for year 2022.

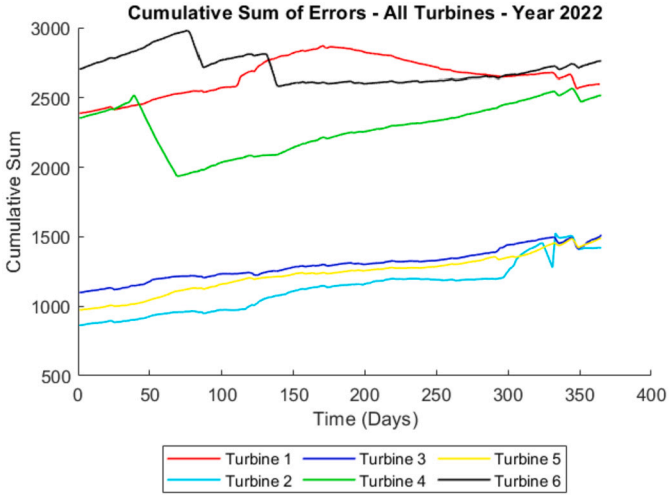

Fig. 24. All turbines - Cumulative sum of the temperature differences continuing from previous year for year 2022.

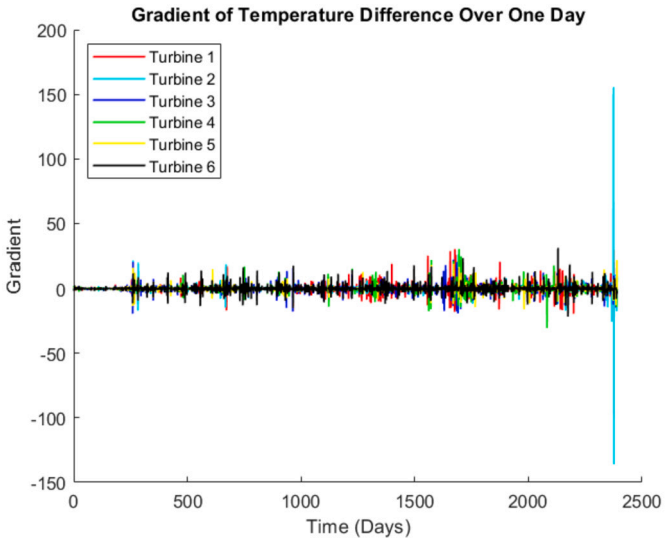

Fig. 25. Gradient of temperature difference for all turbines per day.

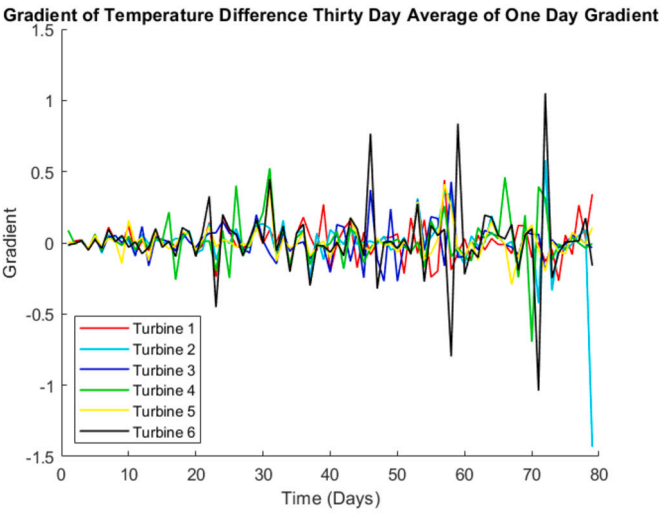

Fig. 26. Gradient of temperature difference for all turbines as per every 30 days.

The additional analysis that is carried out with regards to calculating the gradient of the temperature difference of all the turbines, as shown in Figs. 11 and 12, to see if the gradient increases the closer you get to the failure. Fig. 25 shows the results of calculating the gradient over one day and Fig. 26 uses the gradient value calculated per day, to average the value over thirty days. These graphs show that by averaging over thirty days, the temperature trends appear smoothed out. Fig. 25 suggests that the rear generator bearing in Turbine 2 has obviously suffered a drastic temperature rise within a short time, indicating a different failure type compared to that observed in the other turbines – this component failed in day 2370. With regards to Fig. 26, Turbine 2 failed in November, which equates to day 79, Turbine 4 failed in February, which equates to day 69 and the proactive replacement in Turbine 1 occurred in June, which equates to day 73.

4.3. Component life predictions

The aim of this final analysis, as discussed in Section 3.2, is to calculate the moving average in order to see if there is an obvious threshold, in which if the turbine crosses this, then a component's end of life is near and whether it can be predicted.

As mentioned earlier, Turbines 1, 4 and 6 follow a very similar trend and it is known that two of the Turbines, both 1 and 4, required the

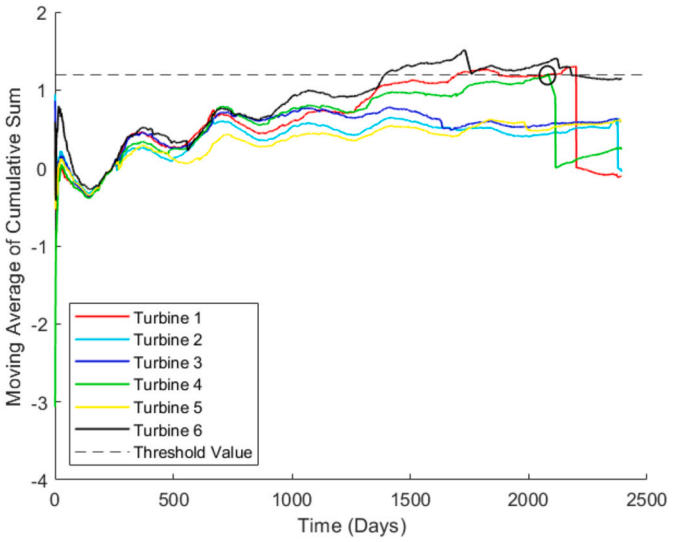

Fig. 27. Moving average of the cumulative sum.

generator NDE bearing to be replaced. From Fig. 27, on the day that Turbine 4 failed, the value of the moving average of the cumulative sum is 1.2. Turbine 1 also crosses this threshold value, around the same time Turbine 4 failed and then went on to have the same component replaced approximately four months later, although we do not have any insight as to why this component was replaced proactively. Turbine 6 crosses this threshold value much earlier in March 2020 and then approximately eleven months later, at the beginning of February 2021 scheduled maintenance was carried out, which again we do not have detailed information on. Therefore, it can be predicted that a threshold value of approximately 1.2, may indicate that a component is coming to the end of it's life in this wind farm. The advantage of the proposed moving average cumulative sum of temperature difference, over the cumulative sum, is that the values of the latter are dependent on the length of time of monitoring up to any given time. However, the former gives the current fraction or rate of accumulated temperature accumulation values at any time. As such, through extrapolating the trend of the moving average cumulative sum, it will be feasible to predict when the moving average will exceed the threshold, which turns out to be the component's end of life. It is noted that the method is restricted to start the monitoring, where the specific components are in the healthy state. While the mentioned extrapolation is outside the scope of this work, proposing this indicator followed by this discussion is aimed to provide a means for end of life prediction for turbine operators, and informing the requirement for additional condition monitoring to possibly extend the service life of drivetrain components.

5. Conclusion

The aim of this paper, was to develop a method to utilize large amounts of annual SCADA temperature data to investigate possible lifetime extension of the drivetrain, by detecting any growing trends in temperature difference, which could indicate that a component is reaching the end of it's life. It was determined that by applying a regression tree ensemble model, using three SCADA input parameters: power, rotor speed and nacelle temperature, along with a component temperature, to wind farm data spanning multiple years, the predicted component temperature could be calculated, which could then be compared to the actual temperature.

From the dataset which was used to test the proposed method, the rear generator bearing was identified as the component which was more vulnerable to fail. The results i.e. temperature difference between the actual and predicted temperatures and cumulative sum of the temperature differences, for this component, for all turbines across all years, was not so conclusive for those rear generator bearings that failed due to operating at higher temperatures over a long period (i.e. Turbine 4), but it can be helpful to identify those components that undergo sudden, sharp temperature rises such as in Turbine 2 which shortly failed after that incident. The final set of results i.e. the moving average of the cumulative sum, found a suitable threshold value of 1.2. Although three turbines crossed this threshold value and either failed or underwent maintenance/downtime, the time between crossing this point and failing varied.

In conclusion, a method to employ SCADA data for life extension has been proposed and has been tested on real life wind farm SCADA data, to try and predict when a component is going to reach it's end of life. In line with earlier research on SCADA data, the results suggest that using only SCADA temperature data, may not be a good indicator for estimating the remaining useful life long in advance, [40], [41], however, the results of this paper provide a method which can help the operator to identify problematic components over the year, from historical data or those which need to be replaced in order to use the drivetrain in a longer run.

6. Future work

As part of the future work, it would be interesting to extend the proposed method to take the model prediction offset/model uncertainty into account. The offset between the actual and predicted temperatures can be calculated, similar to the values in Table D.3. It would be important to determine this offset, to quantify the uncertainty that the predictor model will introduce in the statistics of life estimate results.

Further intriguing work, could be applying the method to a set of data with very little information, other than knowing that there was a failure, as well as using both SCADA and condition monitoring data, to see if a more accurate prediction can be found.

CRediT authorship contribution statement

Kelly Tartt: Writing – review & editing, Writing – original draft, Project administration, Methodology, Investigation, Formal analysis, Conceptualization. **Abbas Mehrad Kazemi-Amiri:** Writing – review & editing, Supervision, Conceptualization. **Amir R. Nejad:** Writing – review & editing, Supervision, Conceptualization. **James Carroll:** Writing – review & editing, Supervision. **Alasdair McDonald:** Supervision.

Declaration of competing interest

The authors declare that they have no known competing financial interests or personal relationships that could have appeared to influence the work reported in this paper.

Data availability

I have shared the link to the dataset in the Acknowledgement Section.

Acknowledgements

Thanks go to the EPSRC for supporting this work through the EPSRC Centre for Doctoral Training in Wind and Marine Energy Systems and Structures (Grant Number EP/S023801/1).

Thanks also goes to Charlie Plumley and Cubico Invest for releasing the Kelmarsh wind farm dataset (https://zenodo.org/records/5841834) and providing support.

Appendix A. Summary of turbine downtime

In this appendix, Tables A.1 and A.2 are presented.

Table A.1
Summary of the scheduled downtime for each Turbine.

	2020 - Downtime Hours		2021 - Downtime Hours		2022 - Downtime Hours	
Turbine	Total	Max	Total	Max	Total	Max
1	30		29		101	25 (June)
2	62	49 (Dec)	26		218	165 (Nov)
3	20		122	77 (Nov)	40	
4	21		36		710	673 (Feb-Mar)
5	14		309	260 (Nov)	58	27 (Oct)
6	23		642	600 (Feb-Mar)	32	

Table A.2
Summary of the forced outage for each Turbine.

	2020 - Downtime Hours		2021 - Downtime Hours		2022 - Downtime Hours	
Turbine	Total	Max	Total	Max	Total	Max
1	57	28 (Mar)	118	92 (July)	31	
2	41		3		66	48 (Nov)
3	76	51 (Oct)	21		3	
4	72	48 (Aug)	12		61	60 (Feb)
5	30		300	240 (Nov)	32	
6	45		118	77 (Feb)	605	221 (Mar)

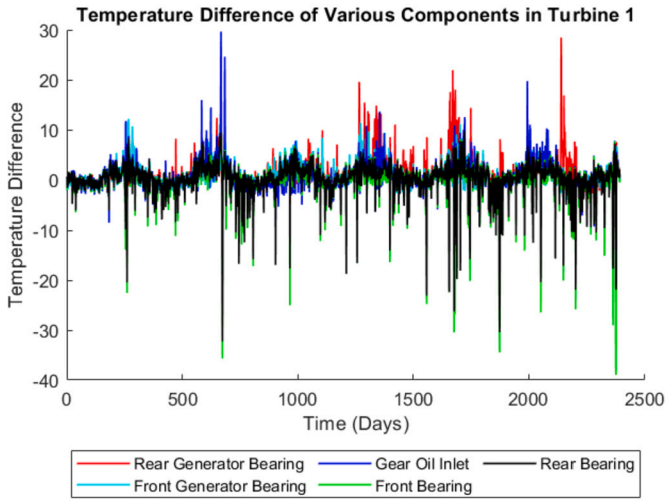

Fig. B.28. Temperature differences for various components in Turbine 1.

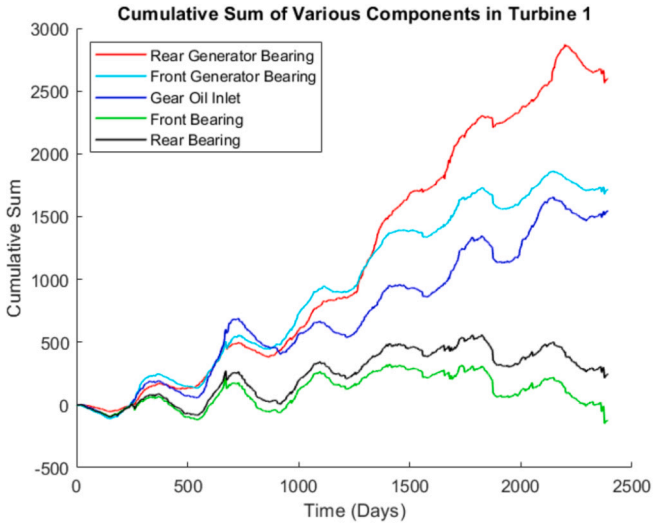

Fig. B.29. Cumulative sum of the temperature differences for various components in Turbine 1.

Appendix B. Graphs showing the results of various components for Turbines 1-3, 5 and 6

In this appendix, Figs. B.28–B.37 are presented.

Appendix C. Graphs showing the results of temperature difference and cumulative sum for Turbines 3, 5 and 6

The other turbine which follows a similar trend to Turbines 1 and 4 is Turbine 6. Figs. C.38 and C.39 show anomalies at both the start of 2021 and 2022. Table A.1, shows 600 hours of scheduled maintenance in February and March 2021, in which once the turbine was back online the temperature difference had reduced. Table A.2 shows 221 hours of forced outage in March 2022 due to pitch motor failure and a pitch fault.

Fig. 12 shows that the remaining two (2) turbines, Turbine 3 and 5 appear to follow the same trend as Turbine 2 and a more detailed look at each one, as shown in Figs. C.40–C.43 shows some anomalies.

Turbine 3 shows an anomaly towards the end of 2020. The anomaly in year 2020 shows decreasing cumulative sum trend (colder temperatures) and the cumulative sum trends of the years seem to be more or less similar in Figs. C.40 and C.41. Aligned with this, for this turbine no failure was reported.

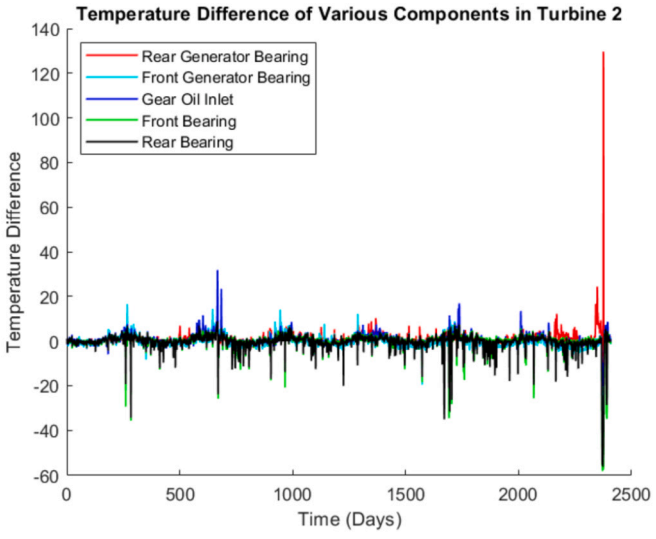

Fig. B.30. Temperature differences for various components in Turbine 2.

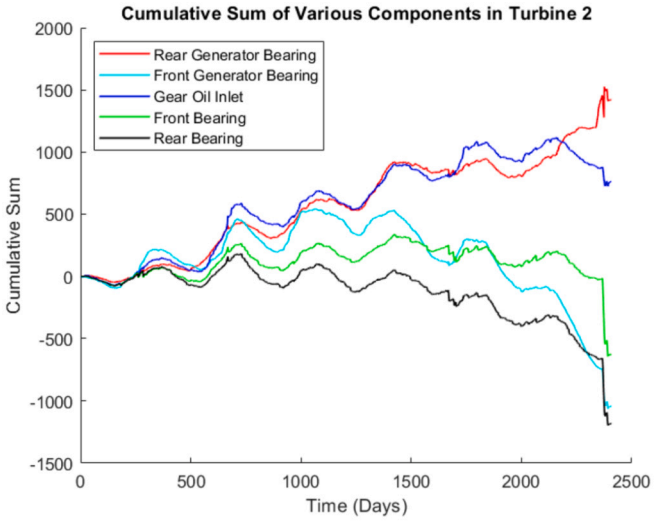

Fig. B.31. Cumulative sum of the temperature differences for various components in Turbine 2.

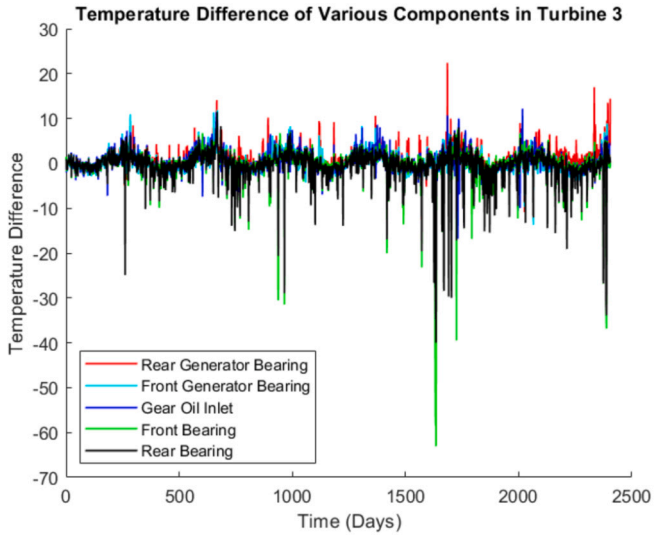

Fig. B.32. Temperature differences for various components in Turbine 3.

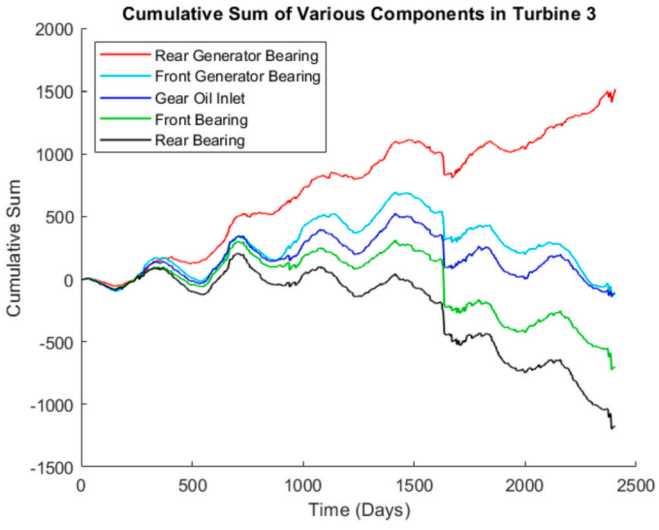

Fig. B.33. Cumulative sum of the temperature differences for various components in Turbine 3.

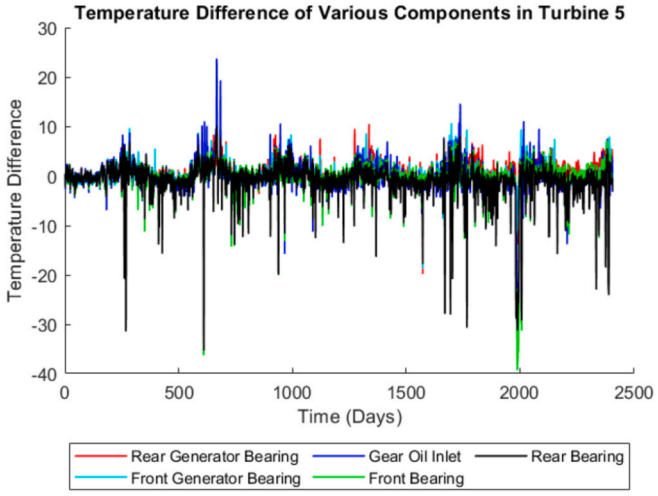

Fig. B.34. Temperature differences for various components in Turbine 5.

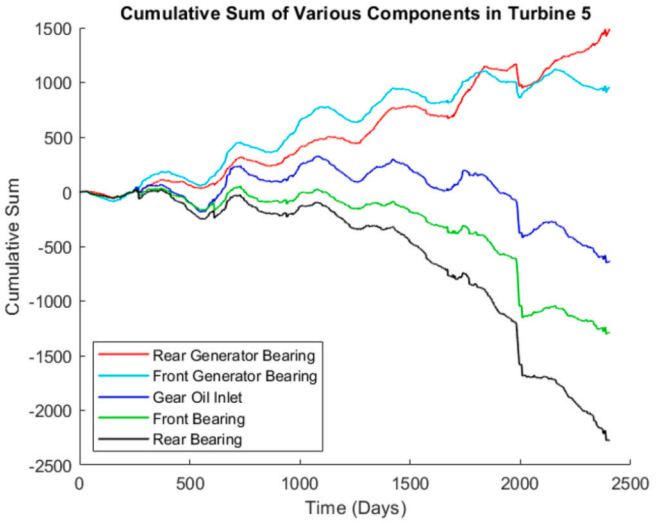

Fig. B.35. Cumulative sum of the temperature differences for various components in Turbine 5.

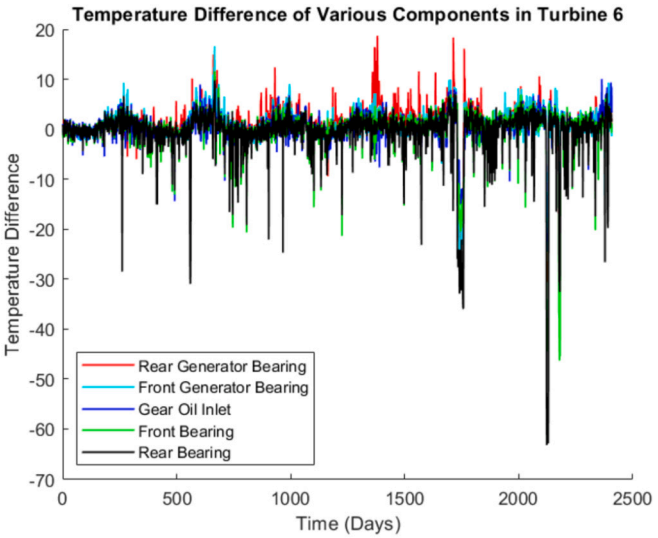

Fig. B.36. Temperature differences for various components in Turbine 6.

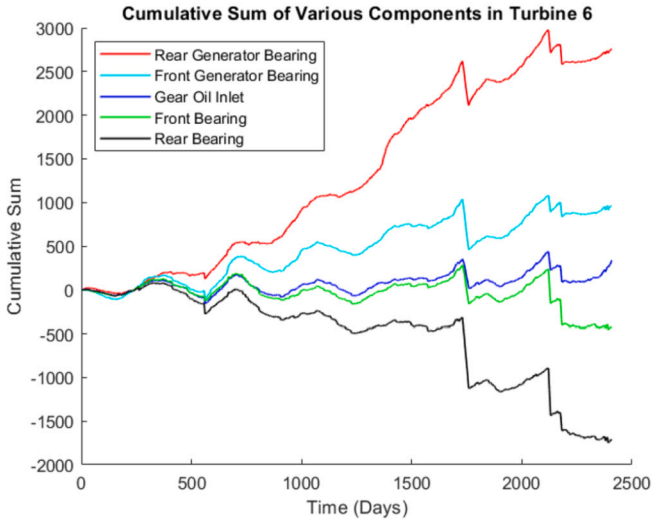

Fig. B.37. Cumulative sum of the temperature differences for various components in Turbine 6.

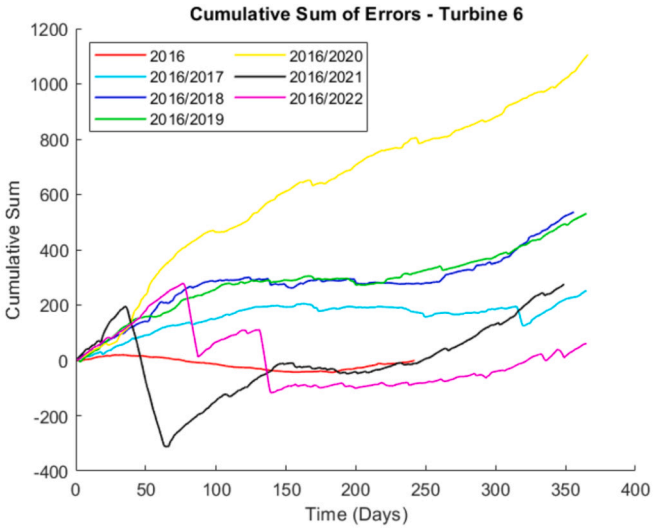

Fig. C.38. Turbine 6 - Cumulative sum of the temperature differences.

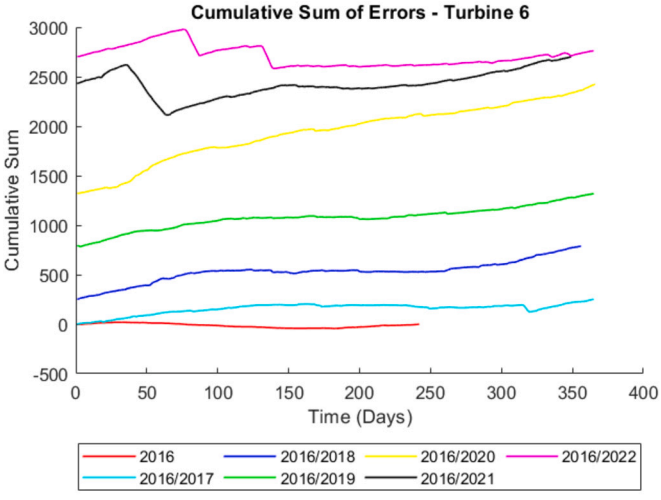

Fig. C.39. Turbine 6 - Cumulative sum of the temperature differences continuing from previous year.

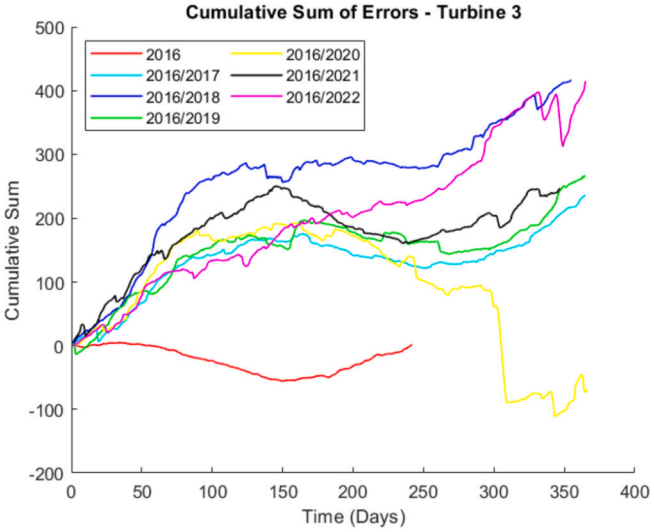

Fig. C.40. Turbine 3 - Cumulative sum of the temperature differences.

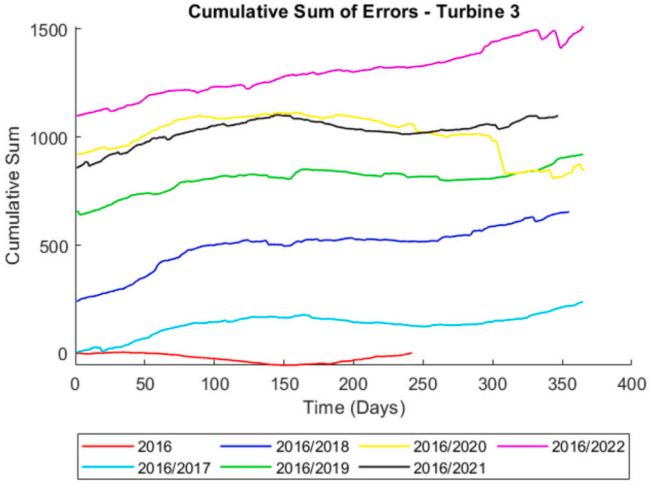

Fig. C.41. Turbine 3 - Cumulative sum of the temperature differences continuing from previous year.

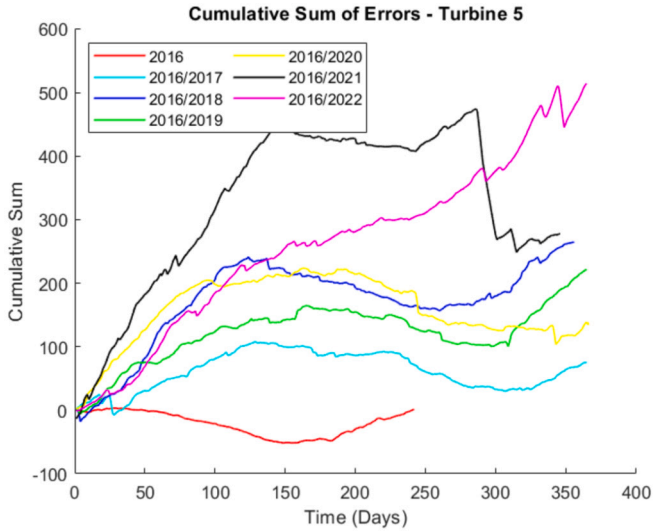

Fig. C.42. Turbine 5 - Cumulative sum of the temperature differences.

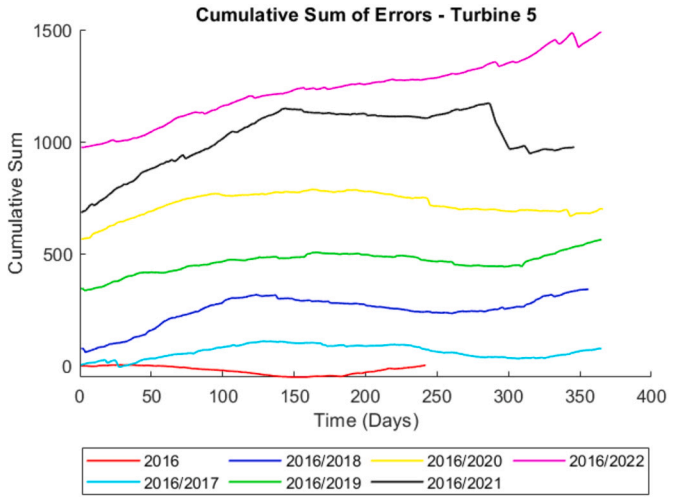

Fig. C.43. Turbine 5 - Cumulative sum of the temperature differences continuing from previous year.

With regards to Turbine 5, although some anomalies start in 2021 with a rising trend but insignificant cumulative sum values are perceived if comparing Fig. C.43 with Fig. C.39.

Appendix D. Table showing the percentage offset values for each turbine to determine the model uncertainty

The average offsets for each turbine are shown in Table D.3. These values have been calculated by taking both the mean and median values for both the predicted and actual component temperatures, for the "healthy" data and determining the percentage difference or offset.

Table D.3
Average offset/uncertainty percentage of the model for each turbine.

	Turbine Number					
	1	2	3	4	5	6
Offset (Mean)	-2.1E-12	5.8E-13	-4.9E-13	-0.02	3.3E-13	-2.8E-13
Offset (Median)	-0.06	-0.31	-0.07	-0.34	-0.34	0.43

References

[1] IEA, World Energy Outlook 2022, Technical Report, 2022.
[2] P. Agreement, Paris agreement, in: Report of the Conference of the Parties to the United Nations Framework Convention on Climate Change (21st Session, 2015: Paris), Retrived December, Volume 4, HeinOnline, 2015, 2017.
[3] H. Government, Net Zero Strategy: Build Back Greener, HM Government, UK, 2021.
[4] R. Plan, Communication from the commission to the European Parliament, the European council, the council, the European economic and social committee and the committee of the regions, European Commission, Brussels, Belgium, 2018.
[5] I.E. Agency, Renewables 2022, Technical Report, 2022.
[6] I. Staffell, R. Green, T. Green, N. Johnson, M. Jansen, January to March 2023: electric insights quarterly, Drax Electric Insights (2023).
[7] T. Taner, A feasibility study of solar energy-techno economic analysis from Aksaray city, Turkey, J. Therm. Eng. 3 (2019) 1.
[8] A.A. Imam, A. Abusorrah, M. Marzband, Potentials and opportunities of solar pv and wind energy sources in Saudi Arabia: land suitability, techno-socio-economic feasibility, and future variability, Results Eng. 21 (2024) 101785.
[9] T. Taner, O.K. Demirci, Energy and economic analysis of the wind turbine plant's draft for the Aksaray city, Applied Ecology and Environmental Sciences 2 (2014) 82–85.
[10] T. Taner, Economic analysis of a wind power plant: a case study for the Cappadocia region, J. Mech. Sci. Technol. 32 (2018) 1379–1389.
[11] T. Taner, The novel and innovative design with using h2 fuel of pem fuel cell: efficiency of thermodynamic analyze, Fuel 302 (2021) 121109.
[12] T. Taner, Energy and exergy analyze of pem fuel cell: a case study of modeling and simulations, Energy 143 (2018) 284–294.
[13] T. Taner, M. Sivrioglu, A techno-economic & cost analysis of a turbine power plant: a case study for sugar plant, Renew. Sustain. Energy Rev. 78 (2017) 722–730.
[14] G.W.E. Council, Global Wind Report 2023, Technical Report, 2023.
[15] J. Tautz-Weinert, S.J. Watson, Using scada data for wind turbine condition monitoring–a review, IET Renew. Power Gener. 11 (2017) 382–394.
[16] K. Tartt, A.R. Nejad, A. Kazemi-Amiri, A. McDonald, On lifetime extension of wind turbine drivetrains, in: International Conference on Offshore Mechanics and Arctic Engineering, vol. 85192, American Society of Mechanical Engineers, 2021, p. V009T09A025.
[17] L. Ziegler, E. Gonzalez, T. Rubert, U. Smolka, J.J. Melero, Lifetime extension of onshore wind turbines: a review covering Germany, Spain, Denmark, and the UK, Renew. Sustain. Energy Rev. 82 (2018) 1261–1271.
[18] A. Turnbull, J. Carroll, S. Koukoura, A. McDonald, Prediction of wind turbine generator bearing failure through analysis of high-frequency vibration data and the application of support vector machine algorithms, J. Eng. 2019 (2019) 4965–4969.
[19] A. Turnbull, J. Carroll, A. McDonald, S. Koukoura, Prediction of wind turbine generator failure using two-stage cluster-classification methodology, Wind Energy 22 (2019) 1593–1602.
[20] M. Gómez, P. Marklund, D. Strombergsson, C. Castejón, J. García-Prada, Analysis of vibration signals of drivetrain failures in wind turbines for condition monitoring, Exp. Tech. 45 (2021) 1–12.
[21] A. Joshuva, V. Sugumaran, A comparative study of Bayes classifiers for blade fault diagnosis in wind turbines through vibration signals, Struct. Durab. Health Monit. 11 (2017) 69.
[22] J. Igba, K. Alemzadeh, C. Durugbo, E.T. Eiriksson, Analysing rms and peak values of vibration signals for condition monitoring of wind turbine gearboxes, Renew. Energy 91 (2016) 90–106.
[23] S. Hussain, H.A. Gabbar, Vibration analysis and time series prediction for wind turbine gearbox prognostics, International Journal of Prognostics and Health Management 4 (2013) 69–79.
[24] W. Teng, X. Ding, S. Tang, J. Xu, B. Shi, Y. Liu, Vibration analysis for fault detection of wind turbine drivetrains—a comprehensive investigation, Sensors 21 (2021) 1686.
[25] Z. Zhang, A. Verma, A. Kusiak, Fault analysis and condition monitoring of the wind turbine gearbox, IEEE Trans. Energy Convers. 27 (2012) 526–535.
[26] J. Carroll, S. Koukoura, A. McDonald, A. Charalambous, S. Weiss, S. McArthur, Wind turbine gearbox failure and remaining useful life prediction using machine learning techniques, Wind Energy 22 (2019) 360–375.
[27] W. Yang, R. Court, J. Jiang, Wind turbine condition monitoring by the approach of scada data analysis, Renew. Energy 53 (2013) 365–376.
[28] A. Murgia, R. Verbeke, E. Tsiporkova, L. Terzi, D. Astolfi, Discussion on the suitability of scada-based condition monitoring for wind turbine fault diagnosis through temperature data analysis, Energies 16 (2023) 620.
[29] Á. Encalada-Dávila, B. Puruncajas, C. Tutivén, Y. Vidal, Wind turbine main bearing fault prognosis based solely on scada data, Sensors 21 (2021) 2228.
[30] J. Herp, M.H. Ramezani, M. Bach-Andersen, N.L. Pedersen, E.S. Nadimi, Bayesian state prediction of wind turbine bearing failure, Renew. Energy 116 (2018) 164–172.
[31] J. Dai, W. Yang, J. Cao, D. Liu, X. Long, Ageing assessment of a wind turbine over time by interpreting wind farm scada data, Renew. Energy 116 (2018) 199–208.
[32] R. Pandit, D. Astolfi, J. Hong, D. Infield, M. Santos, Scada data for wind turbine data-driven condition/performance monitoring: a review on state-of-art, challenges and future trends, Wind Eng. 47 (2023) 422–441.
[33] Y. Feng, Y. Qiu, C.J. Crabtree, H. Long, P.J. Tavner, Monitoring wind turbine gearboxes, Wind Energy 16 (2013) 728–740.
[34] Y. Feng, Y. Qiu, C.J. Crabtree, H. Long, P.J. Tavner, Use of scada and cms signals for failure detection and diagnosis of a wind turbine gearbox, in: European Wind Energy Conference and Exhibition 2011, EWEC 2011, Sheffield, 2011, pp. 17–19.
[35] Z. Yongjie, W. Dongfeng, Z. Junying, H. Yuejiao, Research on early fault diagnostic method of wind turbines, TELKOMNIKA Indonesian Journal of Electrical Engineering 11 (2013) 2330–2341.
[36] B. Corley, J. Carroll, A. Mcdonald, Fault Detection of Wind Turbine Gearbox Using Thermal Network Modelling and Scada Data, Journal of Physics: Conference Series, vol. 1618, IOP Publishing, 2020, p. 022042.
[37] B. Corley, S. Koukoura, J. Carroll, A. McDonald, Combination of thermal modelling and machine learning approaches for fault detection in wind turbine gearboxes, Energies 14 (2021) 1375.
[38] H.-s. Zhao, X.-t. Zhang, Early fault prediction of wind turbine gearbox based on temperature measurement, in: 2012 IEEE International Conference on Power System Technology (POWERCON), IEEE, 2012, pp. 1–5.
[39] X. Zeng, M. Yang, Y. Bo, Gearbox oil temperature anomaly detection for wind turbine based on sparse Bayesian probability estimation, Int. J. Electr. Power Energy Syst. 123 (2020) 106233.
[40] D. Zhang, Z. Qian, Probability warning for wind turbine gearbox incipient faults based on scada data, in: 2017 Chinese Automation Congress (CAC), IEEE, 2017, pp. 3684–3688.
[41] L. Wang, Z. Zhang, H. Long, J. Xu, R. Liu, Wind turbine gearbox failure identification with deep neural networks, IEEE Trans. Ind. Inform. 13 (2016) 1360–1368.
[42] Y. Hu, H. Li, P. Shi, Z. Chai, K. Wang, X. Xie, Z. Chen, A prediction method for the real-time remaining useful life of wind turbine bearings based on the Wiener process, Renew. Energy 127 (2018) 452–460.
[43] R.M.A. Velásquez, Bearings faults and limits in wind turbine generators, Results Eng. 21 (2024) 101891.

[44] C.H.B. Apribowo, S.P. Hadi, F.D. Wijaya, M.I.B. Setyonegoro, et al., Early prediction of battery degradation in grid-scale battery energy storage system using extreme gradient boosting algorithm, Results Eng. 21 (2024) 101709.
[45] B. Ratner, The correlation coefficient: its values range between + 1/- 1, or do they?, J. Target. Meas. Anal. Mark. 17 (2009) 139–142.
[46] A.R. Nejad, Z. Gao, T. Moan, Fatigue reliability-based inspection and maintenance planning of gearbox components in wind turbine drivetrains, Energy Proc. 53 (2014) 248–257.
[47] A.R. Nejad, Y. Guo, Z. Gao, T. Moan, Development of a 5 mw reference gearbox for offshore wind turbines, Wind Energy 19 (2016) 1089–1106.
[48] K. Tartt, A. Kazemi-Amiri, A. Nejad, A. McDonald, J. Carroll, Development of a Vulnerability Map of Wind Turbine Power Converters, Journal of Physics: Conference Series, vol. 2265, IOP Publishing, 2022, p. 032052.
[49] C. Plumley, Kelmarsh wind farm data (0.1.0) [Data set], Technical Report, 2022.
[50] B. Energy, Kelmarsh, Technical Report, 2022.